

**High Performance 3D Geophysical Imaging and 4D Time-Lapse Monitoring of Subsurface Contamination and Associated Processes at the Hanford Site – 14362**

Tim Johnson \*, Mike Truex\*, Jon Thomle\*, Chris Strickland\*, Dawn Wellman \*, John Zachara\*, Dale Rucker \*\*\*, R. Douglas Hildebrand \*\*, Roelof Versteeg \*\*\*\*

\* Pacific Northwest National Laboratory

\*\* US DOE-RL

\*\*\* hydroGEOPHYSICS, Inc.

\*\*\*\* Subsurface Insights

**ABSTRACT**

Electrical Resistivity Tomography (ERT) is a method of remotely imaging the bulk electrical conductivity distribution of the subsurface. ERT imaging is useful for environmental applications because electrical conductivity is governed by many of the physical and chemical properties of interest in contaminated subsurface environments. Over the past 10-15 years, ERT survey instrumentation has advanced rapidly, enabling large amounts of data to be collected quickly and autonomously, and providing the opportunity to characterize the subsurface and monitor subsurface properties at high resolution in space and time. In this paper, we demonstrate how high performance parallel computing resources and advanced ERT imaging techniques have been applied at the Hanford Site to 1) characterize the 3D distribution of vadose zone contamination beneath former waste infiltration galleries at the Hanford B-Complex, 2) monitor engineered vadose zone desiccation for contaminant immobilization in 4D at the Hanford BC Cribs and Trenches Area, and 3) monitor infiltration of Columbia River water into the contaminated aquifer underlying former waste infiltration galleries at the Hanford 300 Area.

**INTRODUCTION**

Over the past 10 to 15 years, commercially available ERT data collection hardware has advanced rapidly, particularly for environmental applications, providing the opportunity to image the subsurface at high resolution over large spatial scales, and enabling subsurface processes to be autonomously monitored through time-lapse ERT imaging. Due to the computational demands of processing such large data sets, the full potential of ERT imaging provided by modern day ERT hardware is often unrealized. In order to optimize ERT imaging for large scale subsurface characterization and time-lapse imaging, we have developed E4D, the first distributed memory parallel ERT inversion code designed specifically for 3D and 4D (i.e. time-lapse) ERT imaging. Herein we demonstrate several applications of high performance ERT for imaging subsurface contamination or understanding properties and processes governing contaminant movement at the Hanford Site.

While in operation large amounts of highly saline low-level radioactive waste were released into shallow infiltration galleries throughout Hanford's Central Plateau and River Corridor. There were also several unplanned releases from failed high-level single-shell waste storage tanks, although in much smaller quantities. The resultant highly-conductive deep vadose zone contamination within Hanford's low-conductivity sands and gravels provides an excellent target for ERT imaging. We demonstrate the 3D inversion of a massive ERT data set collected to image deep vadose zone contamination beneath the Hanford Site B-Complex. Imaging results reveal previously unrealized detail concerning 3D contaminant migration and distribution, and are informing site operators concerning the origin of a nitrate groundwater plume emerging from

beneath the BY-Cribs.

By repeatedly collecting ERT surveys in the same location, 3D changes in bulk conductivity associated with subsurface processes may be produced as snapshots, providing a time sequence of images in a process known as time-lapse 3D, or 4D imaging. At the Hanford 300 Area, located adjacent to the Columbia River, changes in river stage driven by upstream dam operations control river water intrusion and retreat from the unconfined aquifer underlying former waste infiltration ponds and trenches. This groundwater river-water interaction governs uranium release from 300 Area sediments, and plays an intimate role in uranium transport to the river. River water at the 300 Area is less electrically conductive than groundwater, and thereby serves as a natural tracer providing a conductivity contrast for ERT imaging. Based on this, we used 4D ERT to monitor river water intrusion into the 300 Area south process ponds and sanitary leach trenches over an area 350m by 350m for approximately 6 months at a time resolution of 4 images per day. Furthermore, the entire processes from data collection to processing and database archiving was automated and executed in real time, demonstrating a capability for long term 4D autonomous subsurface monitoring using ERT imaging. Results of this effort revealed both the temporal and spatial extent of river water intrusion into the 300 Area during high stage, providing critical information concerning a primary mechanism governing uranium transport at the site.

We begin with a brief overview describing how ERT data are collected and used to reconstruct and image of subsurface bulk conductivity. We then show why bulk subsurface conductivity is a useful metric in contaminated subsurface applications by discussing how it is governed by physical and chemical properties that define contaminants and govern contaminant behavior. We finish by demonstrating several applications of high-performance ERT used to image contaminant distribution and study processes governing contaminant behavior at the Hanford Site.

## **ELECTRICAL RESISTIVITY TOMOGRAPHY PRIMER**

The objective of ERT is to image the resistivity, or equivalently the reciprocal of resistivity, the conductivity, of the subsurface. There are two primary parts of ERT, the survey and the inversion. The survey is where the data are collected, and the inversion is where the data are processed to produce an image of subsurface conductivity (or resistivity). The ERT survey consists of an array of electrodes (i.e. metallic rods) that are connected to survey instrumentation and used to either inject electrical current into the subsurface or to measure the subsurface electrical potential (i.e. the voltage) generated during current injection. The electrodes may be installed on the surface or beneath the surface (i.e. in boreholes) and are strategically arranged to optimize imaging resolution within the target region of the subsurface. A single measurement is made when current is injected between two electrodes, the current source and sink, and the resulting voltage is recorded between two other electrodes, the positive and negative potential electrodes. Survey instrumentation are able to access each electrode as either source or sink, and many measurements are collected in strategic configurations meant to optimize imaging resolution achieved during the inversion phase. ERT surveys typically consist of hundreds to tens of thousands of measurements depending on the number of electrodes.

During the inversion phase, measurements collected during the survey phase are used within a complex computational algorithm to reconstruct, or image the subsurface electrical conductivity distribution governing the survey measurements. The relationship between subsurface and conductivity and potential during current injection is described by the Poisson equation,

$$\nabla \cdot \sigma \nabla \phi = I$$

eq. 1

where  $\sigma$  (S/m) represents the subsurface conductivity,  $\phi$  (V) represents potential, and  $I$  (A) represent current magnitude. A numerical model algorithm is used to model the voltage responses observed for the survey configuration and conductivity distribution. During the inversion, the conductivity distribution is modified to vary through space (and time in time-lapse imaging) so that the observed potentials match the modeled potentials. The inversion is computationally demanding and memory intensive, particularly for 3D and 4D applications.

### **ELECTRICAL CONDUCTIVITY OF THE HANFORD SUBSURFACE**

The electrical conductivity of granular materials comprising the near subsurface is controlled by properties that also describe contaminant states or parameters that control contaminant behavior. For example, within the vadose zone, electrical conductivity is highly dependent on pore water saturation, which is also a primary determinant of unsaturated hydraulic conductivity which governs (in part) the mobility of contaminants. In both the vadose zone and saturated zone, electrical conductivity is dependent upon fluid specific conductance, which is in turn governed by ionic strength and therefore contaminant concentration. Bulk conductivity is also dependent upon subsurface porosity, surface area per unit volume, and electrochemical properties at the pore grain interface that may be influenced by contaminant or remediation related precipitation reactions.

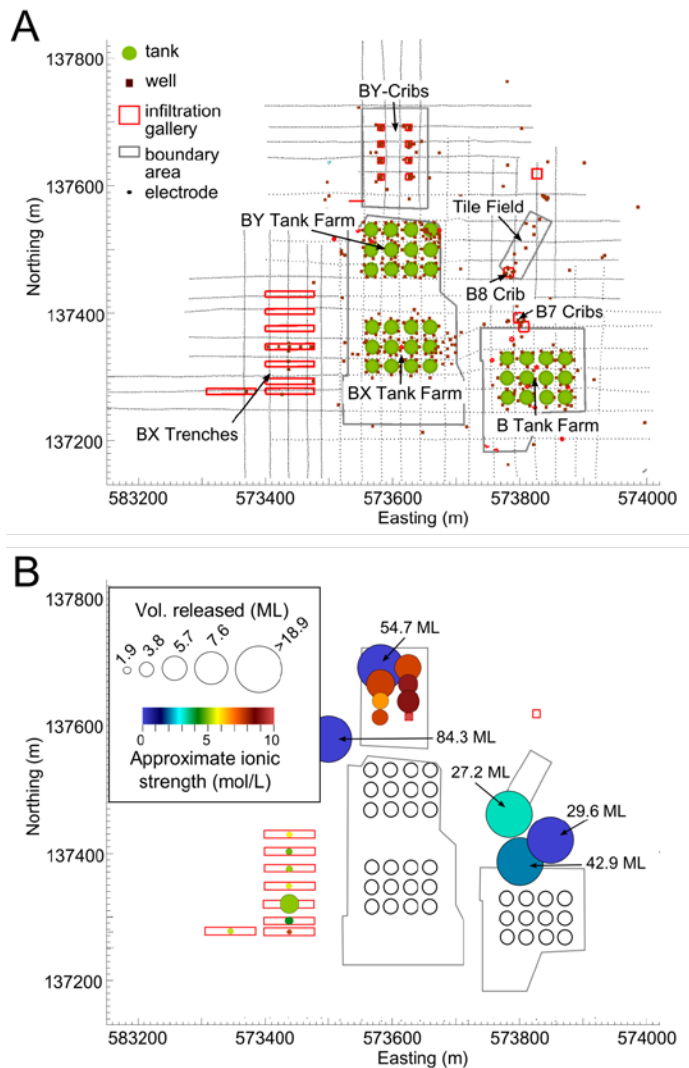
For the specific examples presented in this work, bulk conductivity diagnostic of 1) spatial variations in vadose zone contamination beneath the Hanford B-Complex (pore fluid specific conductance), 2) river water intrusion beneath the Hanford 300 Area (pore fluid specific conductance), and 3) changes in water content during engineered desiccation at the Hanford BC-Cribs and trenches (saturation).

### **3D ERT IMAGING OF VADOSE ZONE CONTAMINATION BENEATH THE B-COMPLEX**

The B-Complex, located in the Hanford 200 East Area, is a former waste disposal facility consisting of 40 single-shell high-level waste (HLW) storage tanks, many of which have leaked or experienced accidental overfill episodes, and several outlying subsurface low-level waste (LLW) infiltration galleries. The waste streams introduced into the vadose zone were highly saline and created contaminated zones of elevated bulk electrical conductivity in contrast to the native low conductivity sands and gravels [1]. This waste poses a significant risk to groundwater quality, and determining the distribution of vadose zone contamination remains one of the most significant challenges limiting remediation and closure of Hanford Site waste disposal facilities [2].

Given the electrical conductivity contrast between contaminated and pristine soils at the B-Complex, a large-scale surface resistivity survey was conducted with the intent of using electrical resistivity tomography (ERT) to map the distribution of subsurface contamination resulting from past waste disposal operations [3]. Figure 1A shows the relative locations of major B-Complex features, including the tank farms, infiltration galleries, wells, and surface electrodes used in the survey. Stainless steel electrodes were laid out in lines parallel and perpendicular to the tanks at a separation of approximately 30 m with an intra-electrode spacing of 6 m and 3 m inside and outside of the tank farm boundaries, respectively. The 36 lines across the site varied in length from 417 to 816 m. Remote electrodes were placed orthogonally to the northeast and northwest approximately 1,900 m from the center of the domain in either direction. The final data set consisted of 208,411 measurements collected on 4,859 electrodes.

Figure 1B shows the locations of the primary waste releases into B-Complex infiltration galleries [4]. The area of the circles represents the volume of waste released in millions of liters (ML), and the color scale represents the approximate ionic strength of the waste. Regions where more than 18.9 ML were released are indicated in text. Higher disposal volumes were generally accompanied by more dilute waste. The exception occurred in the BY-Cribs area, which was subjected to high waste volumes with high ionic strengths. Note that Figure 1B does not include unplanned releases that occurred within the tank farm boundaries. Unplanned releases include spills, leaks, or tank overflow events that are of significantly lower volume, but higher concentration, than the planned releases into the infiltration galleries.



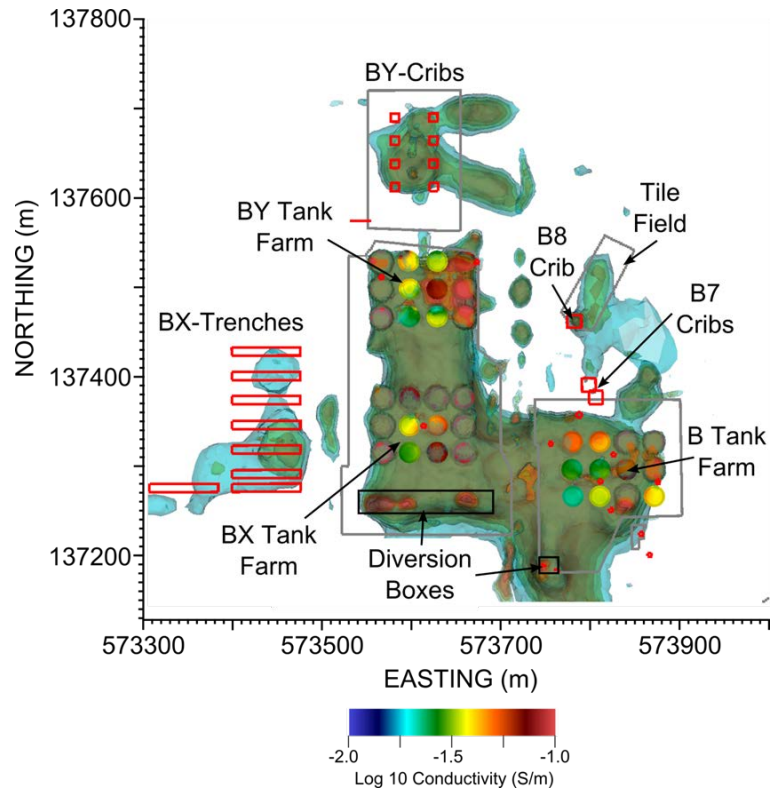
**Figure 1.** A) Plan view of Hanford B-Complex showing locations of storage tanks, infiltration galleries, wells, and electrodes. B) Summary of the major disposal inventories within B-Complex infiltration galleries in terms of volume in millions of liters and approximate ionic strength.

Figure 2 shows a plan view of the ERT inversion results over the entire B-Complex in terms of transparent bulk conductivity isosurfaces [5, 6]. These isosurfaces outline the 3D extent of elevated

bulk conductivity regions that are diagnostic of vadose zone pore water contamination beneath the BX-Trenches, BY-Cribs, B7 and B8 Cribs, and the Tile Field. Elevated conductivities within the tank farm boundaries are primarily dominated by the dense arrays of metallic monitoring wells and tanks. However, the high conductivity regions beneath the waste diversion boxes within the tank farm boundaries are well below the depth of metallic transfer pipes, and given the magnitude of the conductive anomalies, are likely associated with highly contaminated pore water.

According to the waste release inventories shown in figure 1, the BY-Cribs were subjected to high release volumes at elevated concentrations. The majority of these releases were derived directly from tank wastes, and were executed over a 2-year period from 1954-1955 in an effort to create tank storage capacity [7]. Consequently, the BY-Cribs are the most contaminated infiltration galleries within the B-Complex. The discharge inventory into the BY-Cribs is consistent with the ERT inversion results, which show bulk conductivities ranging over approximately 4 orders of magnitude. The ERT images suggest that, in addition to vertical migration beneath the cribs, wastes released into the cribs migrated laterally approximately 100 m in one eastward trending

plume and also in a second south-east trending plume. These observations are consistent with the disposal history shown in 1B, and are site providing site operators with information concerning contaminant distribution and the origin of a contaminated groundwater plume recently emerging from the BY-Cribs Area.



**Figure 2.** Plan view of 3D bulk conductivity distribution beneath the B-Complex with elevated regions outlined by transparent isosurfaces. Elevated bulk conductivity regions originating from the infiltration galleries outside of the tank farms are diagnostic of high ionic strength (e.g., contaminated) pore water in the vadose zone. Bulk conductivity within the tank farm boundaries is largely dominated by the metallic tanks and dry wells, and is therefore inconclusive concerning contaminant distribution. The exception to this includes the regions beneath the diversion boxes, where deep metallic infrastructure is minimal and elevated conductivities are indicative of vadose zone contamination.



into the high-permeability sand and gravel aquifer during high stage. Columbia River water chemistry further facilitates uranium desorption, and thereby enhances uranium release into the aquifer. As stage decreases, groundwater flow again moves toward the river, carrying with it the liberated uranium.

Given the intimate coupling between groundwater/river water interaction and uranium release, extensive geophysical studies have been undertaken to understand the nature of river water intrusion into the 300 Area [11-13]. Slater et al. [11] used waterborne electrical resistivity and induced polarization surveys to map the thickness of the unconfined aquifer at the river bed, which is indicative of paleochannel structures that govern preferential groundwater flows. Building on the work of Slater et al. [11] a 3D array of electrodes was installed over the South Pond Area to image the stage driven inland river water intrusion and retreat from the 300 Area aquifer using 4D Electrical Resistivity Tomography (figures 3 and 4). The objective was to capitalize on the fluid specific conductance contrast between groundwater (~0.04 S/m) and river water (~0.02 S/m), and the corresponding decrease in bulk conductivity within the aquifer as river water replaces groundwater, to image changes in bulk conductivity caused by river water intrusion and retreat.

Using the surface ERT shown in figure 4, four surveys per day were collected from February through November 2013 to image the extend and time of river water intrusion beneath the 300 Area. This period covers the annual high stage spring run off for the Hanford Reach of the Columbia River, which typically peaks in June or July. In this case, the entire imaging process was

automated, from data collection to parallel inversion to database archiving. Figure 4 shows example images of changes in conductivity beneath the 300 Area waste infiltration trenches

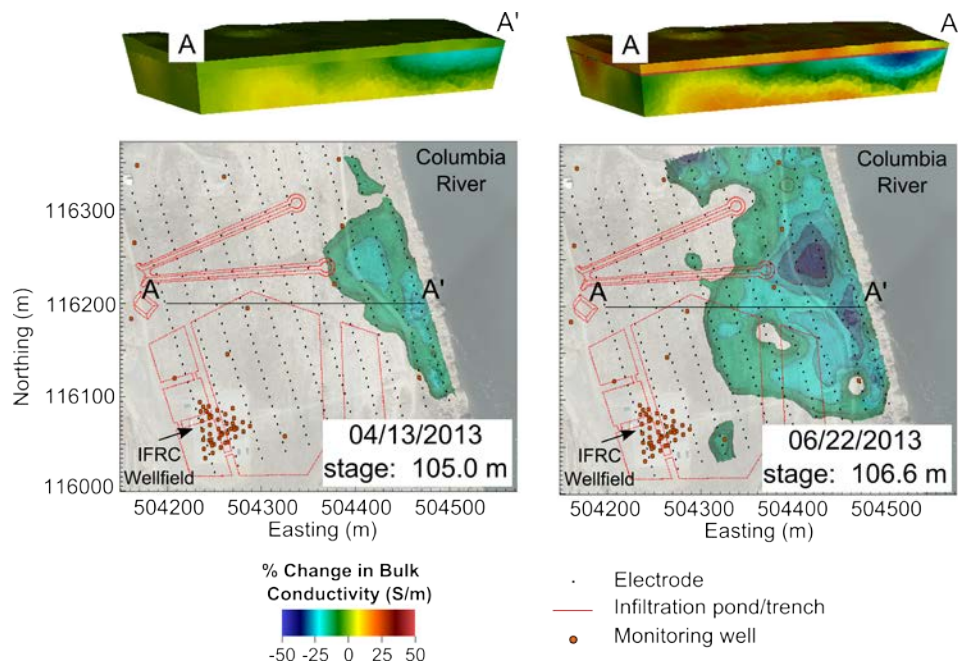


**Figure 4.** 3D Cross-section and plan view ERT images of river water intrusion into the Hanford 300 Area at relatively low stage (105.0 m) and high stage (106.6).

caused by river water intrusion. The heterogeneous nature of intrusion reveal preferred flow pathways and the river water residence time that have a significant influence on uranium desorption and subsequent transport.

#### 4D IMAGING OF ENGINEERED SOIL DESICCATION AT THE HANFORD BC-CRIBS

At the Hanford Site, in situ vadose zone remediation is a potential approach for addressing inorganic and radionuclide contamination located at depths below the limit of direct exposure where remediation is focused on groundwater protection [14]. In 2008, the USDOE initiated a treatability test program to evaluate potential deep vadose zone remedies for protection of groundwater [15], focusing on options to mitigate the vertical movement of contaminants toward the water table. Engineered soil desiccation was investigated as a potential vadose zone remediation technology implemented to reduce the

rate of vadose zone contamination toward the water table (Truex et al., 2013). To apply desiccation, a dry gas is injected into the subsurface. The dry gas evaporates water from the soil until the gas reaches 100% relative humidity and can no longer evaporate water. The desiccation process removes previously disposed and native water from the vadose zone and significantly decreases ability of contaminants to migrate downward within the desiccated region.

The desiccation field test was conducted in the vadose zone at the Hanford Site 200 Area in the BC-Cribs and Trenches (BCCT). The total thickness of the vadose zone beneath the BCCT is about 100 m. Within the BCCT, about 110 million liters of aqueous LLW was infiltrated into multiple engineered cribs and trenches, primarily during the 1950s [7]. The desiccation test consisted a of dipole dry gas injection/extraction well system where gas was passed through the target desiccation zone at a depth interval from approximately 9 to 15 m deep, and a separation of approximately 12 m. Information concerning the distribution of moisture content reduction over time is needed to monitor desiccation performance. Such data are important for determining when desiccation has met treatment goals and when the process can be stopped. Monitoring data can also be used to guide operational decisions, such as adjustments in system flow rates

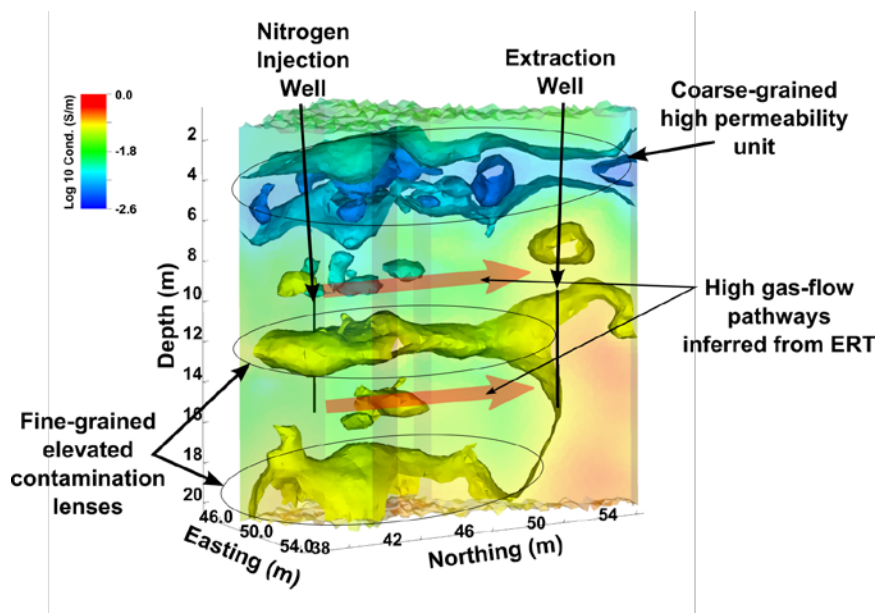


**Figure 5.** Pre-desiccation 3D baseline ERT image showing bulk conductivity along selected iso-surfaces. Higher conductivity lenses are diagnostic of fine-grained, elevated moisture units that tend to harbor contaminated pore water. Lower conductivity lenses represent coarser-grained, higher permeability units that likely provide preferred gas flow pathways.

and injection gas properties. Based on the relationship between bulk conductivity and soil saturation, 4D ERT was used to monitor changes in water content over time within the desiccation zone. In this case, vertical electrodes arrays were placed in boreholes surrounding the injection and extract wells, and used to collect time lapse ERT data during desiccation.

The pre-desiccation ERT imaging results are shown in figure 5. The fine-grained lens with elevated bulk conductivity that straddles the injection well is the target desiccation zone. Such fine-grained lenses are known to have caused lateral contaminant flow in the Hanford vadose zone, and generally exhibit elevated moisture content and contaminant levels when located beneath infiltration galleries. Zones with lower bulk conductivity are typically coarser grained and more permeable, and may provide preferred pathways for gas flow.

During the desiccation test, dry nitrogen gas was injected at a stable flow rate of 510 m<sup>3</sup>/h from January 17, 2011 through June 30, 2011 (164 days) except during a 13-day interval from April 21 through May 4, 2011 when there was no injection. Extraction of soil gas was maintained for the full test duration at a stable flow rate of 170 m<sup>3</sup>/h. ERT data were collected prior to and during desiccation using 99 electrodes; 11 electrodes equally spaced from 6.25 m to 21.5 m deep in each of 9 sensor wells. The electrical conductivities obtained from the inversions were used to estimate volumetric moisture content at each survey time using an approximation based on Archie's Law [16]. Figure 6 shows time-lapse 3D changes in water content derived from the ERT images at selected times. The images indicate that much of the gas flow occurred below the fine-grained unit shown in figure 5, creating a primary desiccation zone just below the fine-grained lens. The figures also show the progression of the desiccation zone from the injection to the extraction well and the development of an upper desiccation zone near the top of the injection well. For validation, figure 6 also shows a comparison of the ERT derived changes in moisture content to those derived from interpolating neutron moisture logs collected 164 days after the start of injection. Although the relative volumes of the desiccated zones are somewhat different, both the ERT and neutron logs describe the same location and relative progression of the desiccated zone, regardless of the approximations in each estimate (i.e. regularization smoothing and Archie's Law assumptions for ERT, calibration and interpolation errors from neutron logs). Overall, the ERT monitoring demonstrated the capability to accurately and remotely monitor 3D changes in moisture content caused by desiccation. In addition, the approach is scalable to larger applications where well-based neutron monitoring becomes less certain due to the extended distance between monitoring wells.

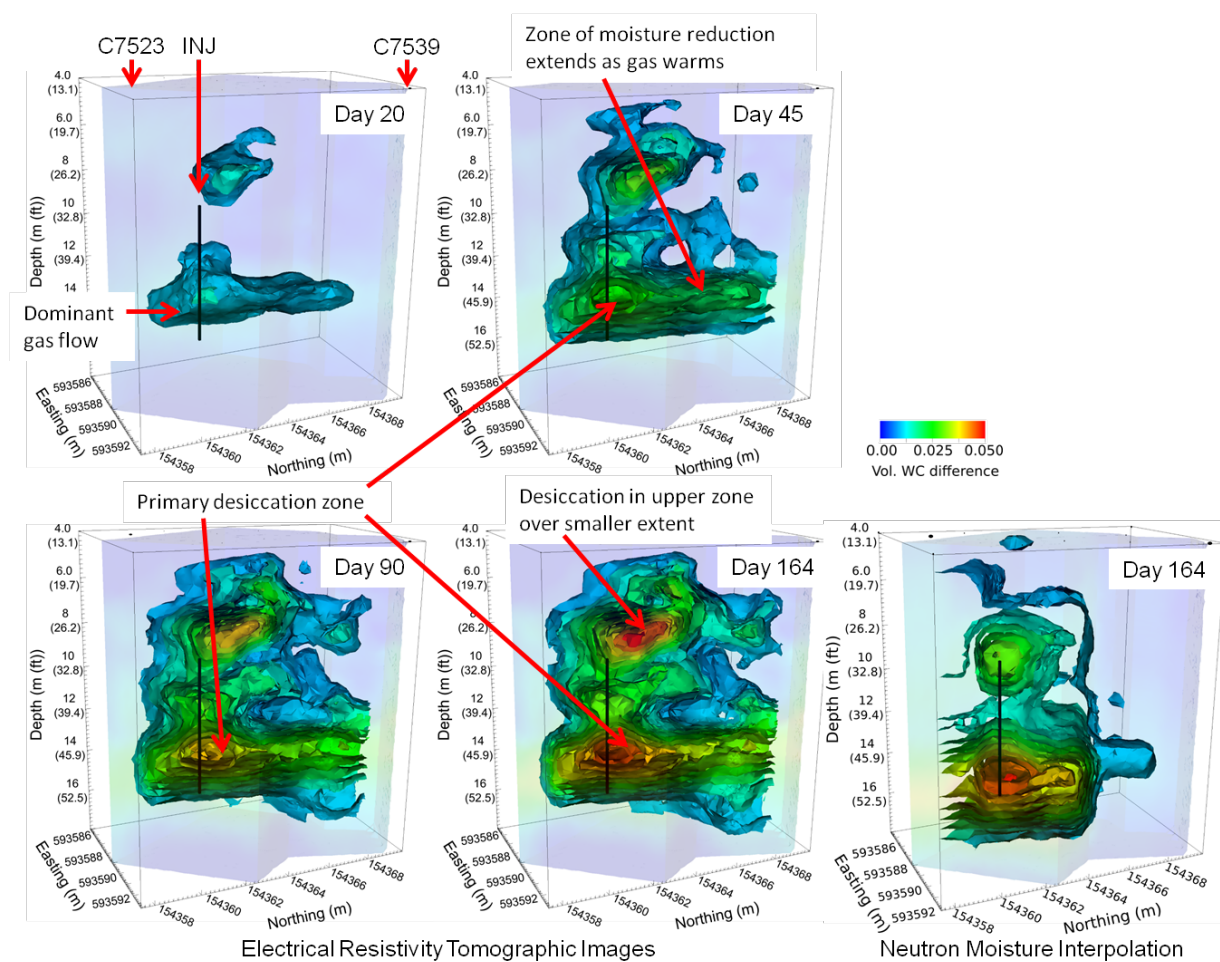


Figure 6. 3-D view of the change in volumetric moisture content over time derived from 3D cross-hole electrical resistivity tomography and neutron moisture data (Truex et al., 2013).

## CONCLUSIONS

ERT is a well proven and robust method of characterizing subsurface structure and monitoring subsurface processes for environmental applications. Advancements in data collection hardware and imaging software are enabling ERT to become practical for large scale 3D characterization and high-resolution 4D time-lapse monitoring applications. The sensitivity of subsurface electrical conductivity to a number of important environmental parameters enables ERT to efficiently provide remote, non-intrusive information at contaminated sites that reduces cleanup cost and risk by reducing uncertainty concerning contaminant and remediation behavior.

## ACKNOWLEDGEMENTS

This work was performed at the Pacific Northwest National Laboratory (PNNL) with funding support from the U.S. Department of Energy-Office of Science, U.S. Department of Energy-Office of Environmental Management, U.S. Department of Energy-Richland Operations Office, and CH2MHill Plateau Remediation Company.

## REFERENCES

1. Lindenmeier, C.W., et al., *Characterization of Vadose Zone Sediment: Borehole C3103 Located in the 216-B-7A Crib and Selected Samples from Borehole C3104 Located in the 216-B-38 Trench Near the BX Tank Farm*, 2002, Pacific Northwest National Laboratory: Richland, WA.
2. DOE/RL, *Long Range Deep Vadose Zone Program Plan*, 2010, United States Department of Energy: Richland, WA. p. 185.
3. Rucker, D., et al., *Surface Geophysical Exploration of the B, BX, and BY Tank Farms at the Hanford Site*, 2007, CH2M HILL Hanford Group, Inc..
4. Williams, J.C., *Liquid radioactive waste discharges from B plant to cribs*, 1996, Westinghouse Hanford Co.: Richland WA.
5. Johnson, T., et al., *Electrical geophysical and geochemical monitoring of in situ enhanced bioremediation*. *Geochimica Et Cosmochimica Acta*, 2010. **74**(12): p. A474-A474.
6. Johnson, T.C. and D.M. Wellman. *Re-inversion of Surface Electrical Resistivity Tomography Data from the Hanford Site B-Complex*. 2013 PNNL-22520]; Available from: <http://www.pnnl.gov/publications/abstracts.asp?report=466710>.
7. DOE/RL, *Groundwater/Vadose Zone Integration Project Background Information and State of Knowledge*, 1999, United States Department of Energy: Richland, WA. p. 251.
8. WHC, *Sampling and analysis of 300-FF-5 operable unit springs and near-shore sediments and river water.*, 1993, Westinghouse Hanford Company: Richland, WA.
9. Williams, M.D., et al., *Three-Dimensional Groundwater Models of the 300 Area at the Hanford Site, Washington State*, 2008, Pacific Northwest National Laboratory: Richland, WA.
10. Peterson, R.E., et al., *Uranium Contamination in the Subsurface Beneath the 300 Area, Hanford Site, Washington*, 2008, Pacific Northwest National Laboratory: Richland, WA.
11. Slater, L.D., et al., *Use of electrical imaging and distributed temperature sensing methods to characterize surface water-groundwater exchange regulating uranium transport at the Hanford 300 Area, Washington*. *Water Resources Research*, 2010. **46**.
12. Johnson, T.C., et al., *Monitoring groundwater-surface water interaction using time-series and time-frequency analysis of transient three-dimensional electrical resistivity changes*. *Water Resources Research*, 2012. **48**.
13. Wallin, E.L., et al., *Imaging high stage river-water intrusion into a contaminated aquifer along a major river corridor using 2-D time-lapse surface electrical resistivity tomography*. *Water Resources Research*, 2013. **49**(3): p. 1693-1708.
14. Dresel, P.E., M.J. Truex, and K. Cantrell, *Remediation of Deep Vadose Zone Radionuclide and Metal Contamination: Status and Issues*, 2008, Pacific Northwest National Laboratory: Richland, WA.
15. DOE/RL, *Deep Vadose Zone Treatability Test Plan for the Hanford Central Plateau*, 2008, U.S. Department of Energy, Richland Operations Office: Richland, WA.
16. Truex, M.J., et al., *Monitoring Vadose Zone Desiccation with Geophysical Methods* *Vadose Zone Journal*, 2013. **12**: p. vzj2012.0147.